JMEPEG (2012) 21:1885–1892
DOI: 10.1007/s11665-011-0108-9

1059-9495/$19.00

A Comparison Between ECAP and Conventional Extrusion for Consolidation of Aluminum Metal Matrix Composite

R. Derakhshandeh Haghighi, S.A. Jenabali Jahromi, A. Moresedgh, and M. Tabandeh Khorshid

(Submitted May 20, 2011; in revised form October 14, 2011)

In this study, two powder consolidation techniques, equal channel angular pressing (ECAP) and extrusion, were utilized to consolidate attritioned aluminum powder and Al-5 vol.% nano-Al_2O_3 composite powder. The effect of ECAP and extrusion on consolidation behavior of composite powder and mechanical properties of subsequent compacts are presented. It is found that three passes of ECAP in tube at 200 °C is capable of consolidating the composite to 99.29% of its theoretical density whereas after hot extrusion of the composite the density reached to 98.5% of its theoretical density. Moreover, extrusion needs higher temperature and pressing load in comparison to the ECAP method. Hardness measurements show 1.7 and 1.2 times higher microhardness for the consolidated composite and pure aluminum after ECAP comparing with the extruded ones, respectively. Microstructural investigations and compression tests demonstrate stronger bonds between the particles after three passes of ECAP than the extrusion. Furthermore, the samples after three passes of ECAP show better wear resistance than the extruded ones.

Keywords ECAP, extrusion, metal matrix composite, powder metallurgy

1. Introduction

Metal matrix composites (MMCs), specially the aluminum-based matrix, have become structural materials that possess light weight, high strength and modulus, low thermal expansion, and good wear resistance (Ref 1, 2). MMCs are promising materials for number of specific applications in aerospace, defense, and automobile industries (Ref 3). MMCs can be reinforced by particles (non-continuous reinforced composites) or fibers (continuously reinforced composites). Compared to continuously reinforced composites, the non-continuous reinforced composites show lower production cost, more adaptable processing methods, higher thermal stability, and better wear resistance (Ref 3, 4). Combination of metallic matrix and ceramic reinforcement like oxides or nitrides leads to the improvement in physical and mechanical properties of composites (Ref 5).

MMCs are manufactured by different techniques. These techniques are classified as (1) liquid phase processes, (2) solid state processes, (3) liquid-solid processing. The first and third groups have some limitations in mixing the two phases thoroughly and the problems due to wettability at matrix-reinforcement interface (Ref 6). Solid state processing such as powder metallurgy techniques (P/M) are used extensively in manufacturing (MMCs). In this technique, the powders are mixed completely and then the powders are consolidated and sintered in the furnace. In order to significantly reduce the percentage porosity during compaction alternative processes such as extrusion (Ref 7, 8) involving high strains are used. Several advantages of powder metallurgy technique can be listed here as, (1) homogeneity of the mixture is well controlled. (2) The composite inherits all the advantages of the rapidly solidified powdered metals. (3) The component is produced in near net-shape dimension (Ref 6). According to Tan and Zhang (Ref 9) when a secondary deformation, like extrusion, with large strain is used, the distribution of reinforcement particles becomes more uniform regardless of matrix and reinforcement particle size and their volume fractions. However, utilization of extrusion as a secondary process on the composites has some limitations. Extrusion reduces the cross section of the material and furthermore it needs extreme extrusion force. Recently, equal channel angular pressing (ECAP) has been used for powder compaction. However, little study has been conducted on powder compaction via ECAP method (Ref 10-14). ECAP is one of the severe plastic deformation techniques with unique advantages such as large strain, no change in cross section, and minimum load requirements. Moreover, the incorporation of second phase components which are not suitable for incorporation during a melting step is easy (Ref 15) and also ECAP permits a variety of deformation configurations by changing the orientation of the billet with respect to the extrusion axis after each pass (Ref 15-17).

Powder compaction by ECAP has been done through the powder in tube (PIT) technique (Ref 18). Applying back pressure within outlet ECAP channel for increasing hydrostatic pressure for better consolidation of the powders is another technique which has attracted attention (Ref 11, 19-21) but applying back pressure may lead to increase of overall pressing loads (Ref 22). Most of the studies have been carried out on the compaction of pure metallic materials such as pure aluminum

R. Derakhshandeh Haghighi and **A. Moresedgh**, Department of Materials Science and Engineering, Science and Research Branch, Islamic Azad University, Fars, Iran; and **S.A. Jenabali Jahromi** and **M. Tabandeh Khorshid**, Department of Materials Science and Engineering, School of Engineering, Shiraz University, Shiraz, Iran. Contact e-mail: derakhshande@shirazu.ac.ir.

(Ref 11) and copper powder (Ref 15) and some on the compaction of composite powders by ECAP like carbon nanotube reinforced MMCs (Ref 23) and most of them focused on true consolidation and mechanical property enhancement. However, negligible efforts were made to compare the capability of ECAP in comparison to conventional extrusion for enhancing the physical and mechanical properties of the aluminum matrix composites. In thus study, efforts were made to consolidate Al-5 vol.% nano-Al_2O_3 by two methods, namely ECAP and conventional extrusion method and to compare the physical and mechanical properties which are attained after each process.

2. Materials and Methods

Nitrogen gas atomized Aluminum powder with mean particle diameter of 45 μm, and α-Al_2O_3 nano-particles with average size of 35 nm were used as starting materials. Aluminum and alumina powder with 5 vol.% Al_2O_3 were mixed in ethanol and vibration treated for 1 h by ultrasonic to separate the agglomerated powder and to help homogenous mixing. The powder mixtures were wet attritioned in pure ethanol slurry in a container with steel balls with a diameter of 5 mm and a rotational speed of 400 rpm for about 500 min with an interruption every 90 min for about 10 min to decrease temperature rise during attritioning operation. The ethanol was removed from the mixture by a pump which operates simultaneously with the attritioning process and after the removal of the ethanol the powder mixture was dried at 150 °C for 90 min.

In order to consolidate the composite powder via ECAP, a copper tube with two plugs, namely rear and front plugs for closing the two ends of the tube, were used and the tube was filled with the attritioned powder. In order to avoid oxidation of the powder a glove box with a controlled atmosphere of argon was utilized and the filling of the tubes was done in this condition. Front and rear plugs were prepared using copper. Geometry and dimensions (in mm) of the tubes used are shown in Fig. 1(a). The PIT was then subjected to multi-pass ECAP, with a 20 ton press and the ram speed of 0.5 mm/s using ECAP die (Fig. 1d) with channel inner and outer angles of 90° and 20° at 200 °C (Fig. 1b). Route B_c—90° clockwise rotation of the specimen after each pass of ECAP is called route B_c—was adopted to study the influence of multi-pass ECAP on the extent of compaction of powders. On the other hand, some of the attritioned powders were compacted uniaxially in a rigid die (Fig. 1c) at compaction pressure of 200 MPa, and then the compacted powder with the initial diameter of 45 mm was sintered at 540 °C in controlled atmosphere for about 60 min following by extrusion in one step at the ratio of 20:1. Using lower temperature for sintering and extrusion was not possible due to existence of weak bonds between particles and disintegration during extrusion.

The density of the materials was measured based on the Archimedes principle using polished samples. The Vickers microhardness (HV) was measured by applying 10 N load for 10 s loading time and taking an average over eight separate measurements. Compression test was carried out for the composite specimens to investigate the strength of the bonds between the particles by cutting the cylinders from the compacted powder with nominal diameter of 10 mm and length of 10 mm. Teflon tape was used around the compression specimens to minimize friction. Due to small-sized specimens which are obtained after ECAP, the tension test was not possible. The wear test was carried out with a pin on ring apparatus, with a 4140 alloy steel disc with hardness of 60 HRC at a sliding speed of 0.33 m/s and loads of 10 and 20 N for a sliding distance of 400 m without lubricant. During testing, the pin specimen was kept stationary while the circular disk was rotated. The composite test sample was clamped in a holder and held against the rotating steel disc. The amount of wear was determined by measuring the weight loss of the samples. Scanning electron microscopy (Leica Cambridge model SEM) and optical microscopy were performed on the cross section of the polished surface, fractured surface, and worn surface of the specimens. For this purpose, after polishing the surface of the sample, they were etched in a solution of 15.5 mL HNO_3, 0.5 mL HF (48%), and 3.0 g CrO_3 in 84.0 mL

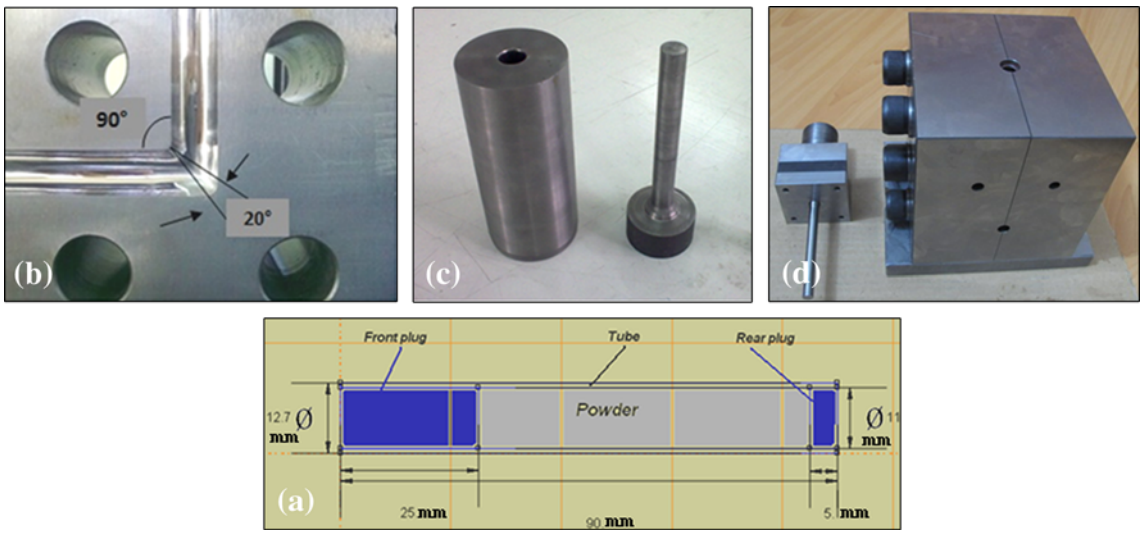

Fig. 1 (a) Geometry and dimensions (in mm) of the tubes used in the study, (b) inner and outer angels of the channels intersection, (c) uniaxial compression die, and (d) ECAP die assembly

H_2O. The specimens were investigated through SEM at different magnification values of 200×, 400×, 1000×, and 25,000×. In order to investigate the densification process, the composite specimens were broken by an impact load using an impact test instrument at room temperature and the fracture surfaces were checked out by scanning electron microscopy.

3. Results and Discussion

SEM micrographs of the severely deformed particles and flattened grains are seen in Fig. 2(b) and the as-received gas atomized aluminum particles which exhibit an irregular shape are presented in Fig. 2(a). It is difficult to consolidate the flaky particles due to formation of bridges and high friction between particles. Figure 3 presents the SEM micrographs of Al-5 vol.% Al_2O_3 after different passes of ECAP which were also investigated in our previous work (Ref 24). It seems that three passes of ECAP is sufficient to eliminate the micropores. After the first pass of ECAP in Fig. 3(a), large micropores with nanometric alumina particles which are agglomerated to decrease their surface energy are seen in aluminum matrix. In the second pass (Fig. 3b), still some micropores exist (solid arrows), especially near the alumina particles but in the third pass (Fig. 3c), the pores are eliminated and nanometric alumina particles (dotted arrows) have good bonding with the matrix material. The amount of porosity (solid arrows) is a bit lower in

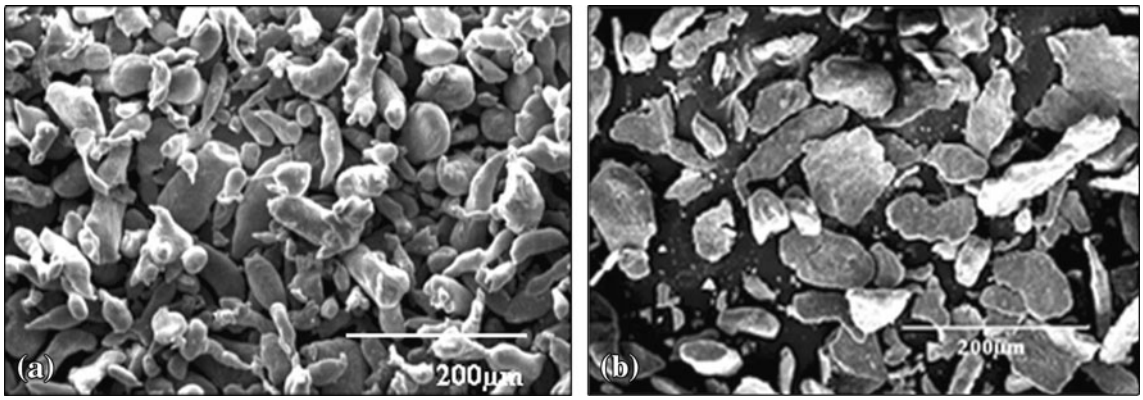

Fig. 2 SEM micrographs of (a) as-received gas atomized aluminum powder and (b) the morphology of the attritioned composite powder

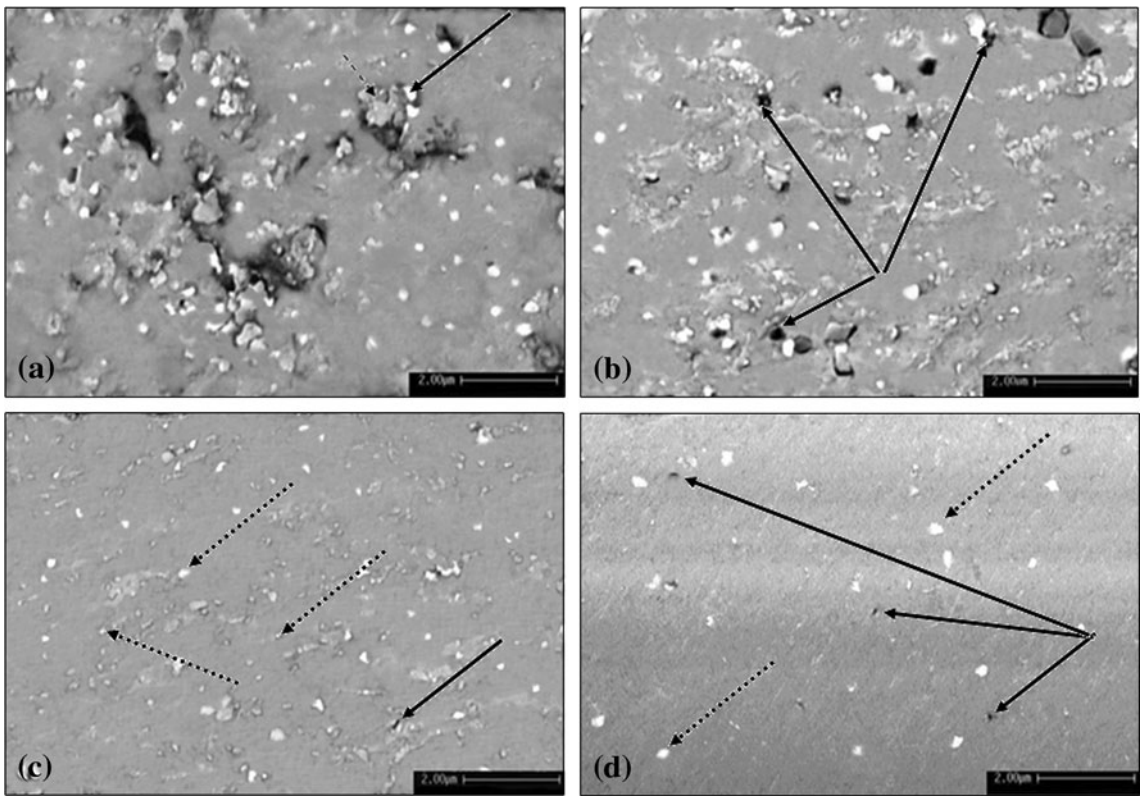

Fig. 3 SEM micrographs of Al-5 vol.% Al_2O_3 composite after (a) first pass of ECAP (bold arrow shows loose alumina and dotted arrow shows loose aluminum powder), (b) second pass of ECAP, (c) third pass of ECAP, and (d) extrusion

the microstructure of the samples after three passes of ECAP in comparison to the extruded samples in Fig. 3(d). Figure 3(d) shows the SEM micrograph of the extruded composite with alumina particles in the aluminum matrix. These alumina particles (dotted arrows) are larger in size than the alumina particles in Fig. 3(c) mainly because of this fact that the declustering occurs due to severe plastic deformation of the clusters during ECAP. In fact smaller particle size is obtained after three passes of ECAP than the extrusion. Extrusion has eliminated the pores but still some pores are visible in the microstructure (solid arrows). However, better distribution of the reinforcement in the matrix was achieved after three passes of ECAP comparing with the extrusion.

Figure 4(a) and (b) presents the optical micrograph of the consolidated composite after the third pass of ECAP and extrusion techniques after etching, respectively. The grains are almost equiaxed and the reduction of grain size after consolidation of the composite via ECAP method is obvious comparing with the extruded sample. Using the linear intercept method, the average grain size for the ECAPed samples was measured as 7 μm, while the average grain size for the extruded composite sample was measured as about 17.3 μm. The alumina particulates could pin grain boundaries and give rise to grain refinement, moreover severe plastic deformation by ECAP introduces the complexity of repetitive passes with varying shear strain planes and accumulation of stored dislocations which promote grain refinement (Ref 25). Table 1 presents the density of the composite and the monolithic aluminum powder after ECAP and conventional extrusion. Density measurements show that the density gradually increases by increasing ECAP passes and a relatively higher density is attained after three passes of ECAP for composite and after two passes of ECAP for pure aluminum comparing with the conventional extrusion. Lapovok (Ref 26) has shown that shear mode of plastic deformation in ECAP leads to a change in pore geometry which is favorable for pore closure under hydrostatic pressure and according to Nagasekhar et al. (Ref 18) the powder undergoes shear deformation due to mechanical interlocking and this cyclic phenomenon causes the compacts to densify close to the theoretical density. It should be noted that pore reduction in ECAP, starts as the front plug undergoes shear deformation. The residual porosity is eliminated when the powder undergoes shear deformation by imposing high level of strain. Furthermore, the densification of the composite powder is harder due to hard nano-alumina powder in comparison to the pure aluminum powder. Figure 5 shows the load-displacement curves for the two techniques.

Because of strain hardening of the tube and the plugs and also the consolidated powder, the load increases by increasing the number of ECAP passes. The highest load is experienced during the front plug extrusion but when the powder undergoes shear deformation the load decreases. However, the load required for extrusion of the composite is completely ascendant and is about 2.5 times higher than the maximum load which is required in the third pass of ECAP. Lower load requirement coupled with low temperature requirement and also elimination of uniaxial die compression before extrusion, seems to reduce the expenses during consolidation of composite powder via ECAP. It is to be noted that comparison of the extrusion force is restricted by unequal technological conditions such as volume

Table 1 The density of the composite and the monolithic aluminum powder after ECAP and conventional extrusion

Consolidation method	Pure Al (2.7 g/cm^3)	Al-5 vol.% Al_2O_3 (2.76 g/cm^3)
First pass ECAP	2.62	2.65
Second pass ECAP	2.7	2.72
Third pass ECAP	…	2.74
Extrusion	2.65	2.72

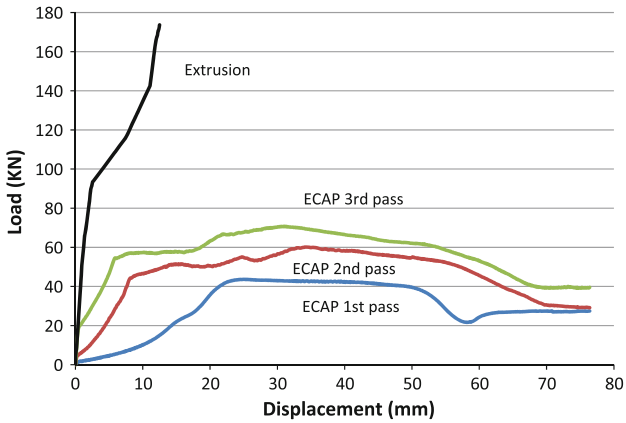

Fig. 5 The load-displacement curves for the ECAP and extrusion techniques

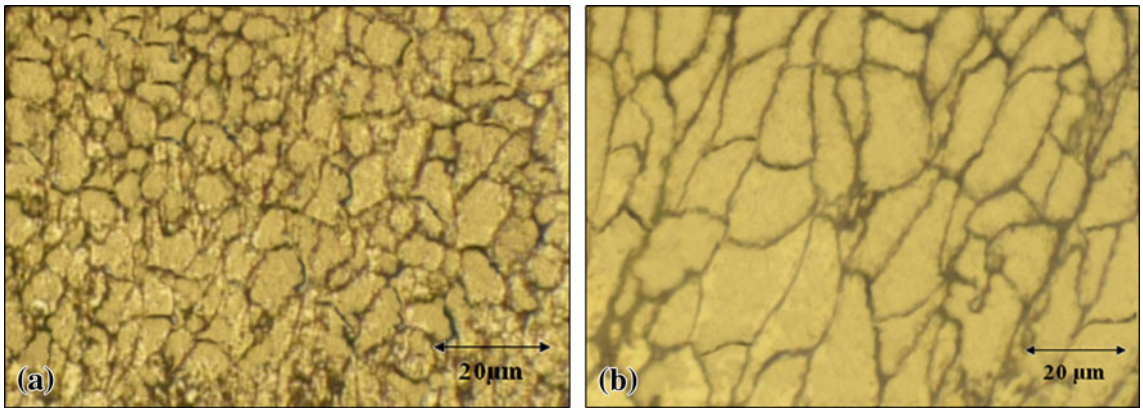

Fig. 4 Optical micrograph of the consolidated composite after (a) third pass of ECAP and (b) extrusion

of compacted material, wall friction, etc. during extrusion and ECAP, thus needs to be considered as approximate (Ref 22). Table 2 indicates the hardness values for different passes of ECAP (Ref 24) and extrusion for the consolidated pure aluminum and the composite. The hardness increases with increasing the number of ECAP passes because of this fact that the powder density increases and the level of accumulative strain enhances after each pass of ECAP. However, the maximum hardness values after extrusion are extremely lower than the ECAPed samples. It is mainly due to higher accumulative strain level and more trapped dislocation density and in fact smaller grain size which is achieved during ECAP comparing with the conventional extrusion. The hardness value after the third pass of ECAP for the composite is about 1.7 times higher than its counterpart after extrusion and about 1.2 times higher for the pure aluminum after second pass of ECAP in comparison to the extruded samples. The higher hardness value of the composite than the pure aluminum is due to the higher amount of hard nano particles in Al-5 vol.% Al_2O_3 which leads to dislocation generation due to thermal expansion mismatch between hard alumina particles and ductile matrix (Ref 27) and also the interaction of the dislocations with the particles which leads to leaving residual dislocation loops around each particle according to Orowan mechanism.

Figure 6 demonstrates the compression true stress-true strain of the consolidated composite after ECAP and extrusion. Compression tests can be helpful to study the barreling and upsetting behavior of the compacts. However, in this study the amount of barreling was not considerable and the test was stopped before considerable shape change and uniform strain was distributed in the specimens. Stronger bonds among particles delay the crack initiation during deformation. ECAP has this capability to consolidate the composite near to its theoretical density with strong bonds among particles after the third pass of ECAP which is obvious from the results of the compression test for the composite. It should be noted that one pass of ECAP is not sufficient for complete consolidation of the composites and the compression specimens fractured prematurely as was demonstrated in our previous work (Ref 24). After the third pass of ECAP good bonds form between the particles and the high compressive strength is obtained in comparison to the extruded samples. The ductility of the extruded composite is about 2.5 times higher than the ECAPed samples, mainly because of disadvantageous texture of the elongated grains angled at ~45° to loading direction as a result of ECAP shearing plane (Ref 22) .The amount of high angle grain boundaries is high in shear bands after ECAP and the shear bands interact with these high angle grain boundaries. The multiplication and interaction and tangling of dislocations occurs during multi-pass ECAP and as the high angle grain boundaries are effective sinks of dislocations, the number of mobile dislocations decreases and in turn ductility decreases (Ref 28). It should be noted that to get high ductility for ECAPed samples, homogenous array of uniform and equiaxed grains separated by high angle grain boundaries is needed (Ref 29) and this happens by increasing the number of ECAP passes to a reasonable value, whereas the textures in which the grains are oriented parallel to the extrusion direction in the extrusion process lead to higher ductility. Lower elastic modulus for extruded samples and the sample after the first pass of ECAP is because of this fact that the elastic modulus is very sensitive against porosity. According to Bjorn Clausen et al. (Ref 30) the elastic modulus of $NiAl_2O_4$ with 3% porosity is 1.5 times greater than the reduced $NiAl_2O_4$ (a composite of Ni and Al_2O_3) with 12% porosity, in fact the residual pores generally cause a decrease of elastic modulus (Ref 31).On the other hand,

Table 2 The microhardness, HV, values for different passes of ECAP and extrusion for the consolidated pure aluminum and the composite

Consolidation method	Pure Al	Al-5 vol.% Al_2O_3
First pass ECAP	49.5	106.1
Second pass ECAP	61.6	134.9
Third pass ECAP	…	143.6
Extrusion	50.2	85.6

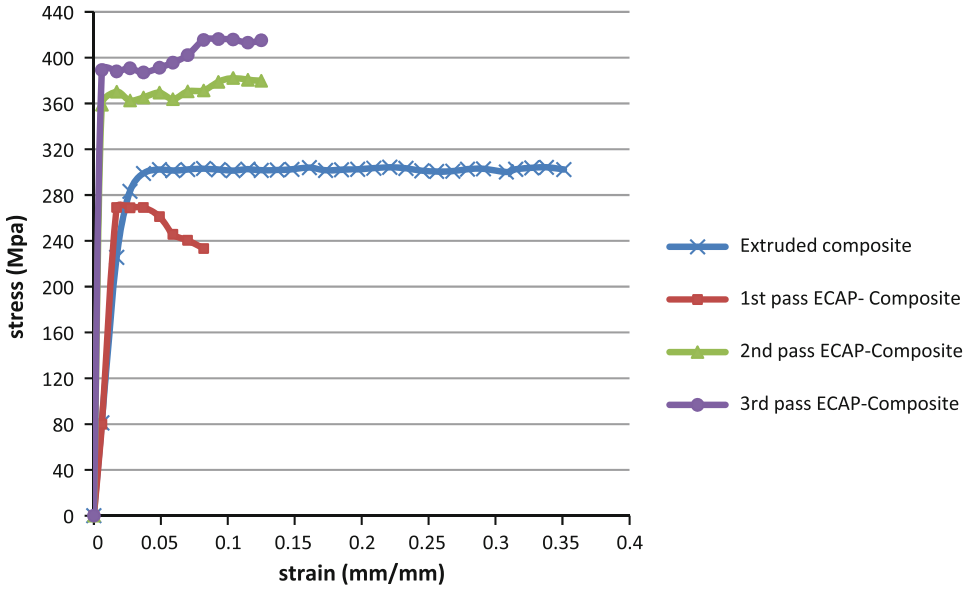

Fig. 6 The compression true stress-true strain of the consolidated composite after ECAP and extrusion

according to Ganesh and Chawla (Ref 32), a definite anisotropy in elastic modulus exists because of more favorable alignment of the Al_2O_3 particles. In ECAP process after the second and the third passes, better distribution and alignment of the particles occurs along a given direction in comparison to the extrusion process so as the majority of the particles align in a specific direction the amount of anisotropy increases for ECAPed samples. It means that, ECAP has this capability to align a larger fraction of the particles in a specific direction so that higher elastic modulus is observed after ECAP than conventional extrusion.

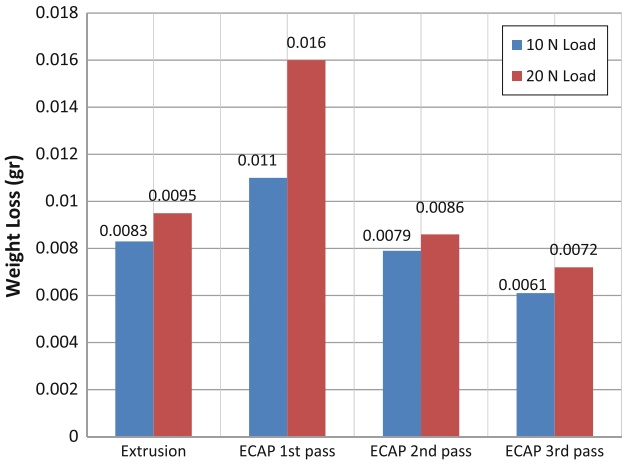

Fig. 7 The weight loss of nano-composite after extrusion and three passes of ECAP, for two normal loads (10 and 20 N) and sliding distance of 400 m

Figure 7 shows the weight loss of nano-composite after extrusion and after three passes of ECAP, for two normal loads (10 and 20 N) and sliding distance of 400 m. As it is seen, the weight loss decreases by increasing the number of ECAP passes due to hardness enhancement and better consolidation of the particles. However, the weight loss is higher for the samples after the first pass of ECAP than the extruded samples. This is because of loose aluminum and alumina particles (dotted and bold arrows in Fig. 3a, respectively) and improper bonds between particles after the first pass of ECAP. The extruded samples show higher weight loss comparing with the ECAPed samples after the second and the third passes of ECAP. In general, the weight loss increases by applying higher loads (20 N). Fig. 8 shows the SEM micrograph of the worn surface of the nano-composite after extrusion and ECAP for the load of 20 N and the sliding distance of 400 m with the velocity of 0.33 m/s.

Figure 8(a) shows the worn surface of the work piece after the first pass of ECAP. This is the result of the wear particle formation which undergoes milling action between the mating surfaces. The increasing hardness of the work hardened wear debris rolling between the mating surfaces and also the weak bonds between the particles give rise to a plowing action to the composite surface, causing microgrooves on the composite worn surface (Ref 33, 34).This is consistent with the results of higher amount of weight loss in Fig. 7 which is obtained for the samples after the first pass of ECAP. By increasing the number

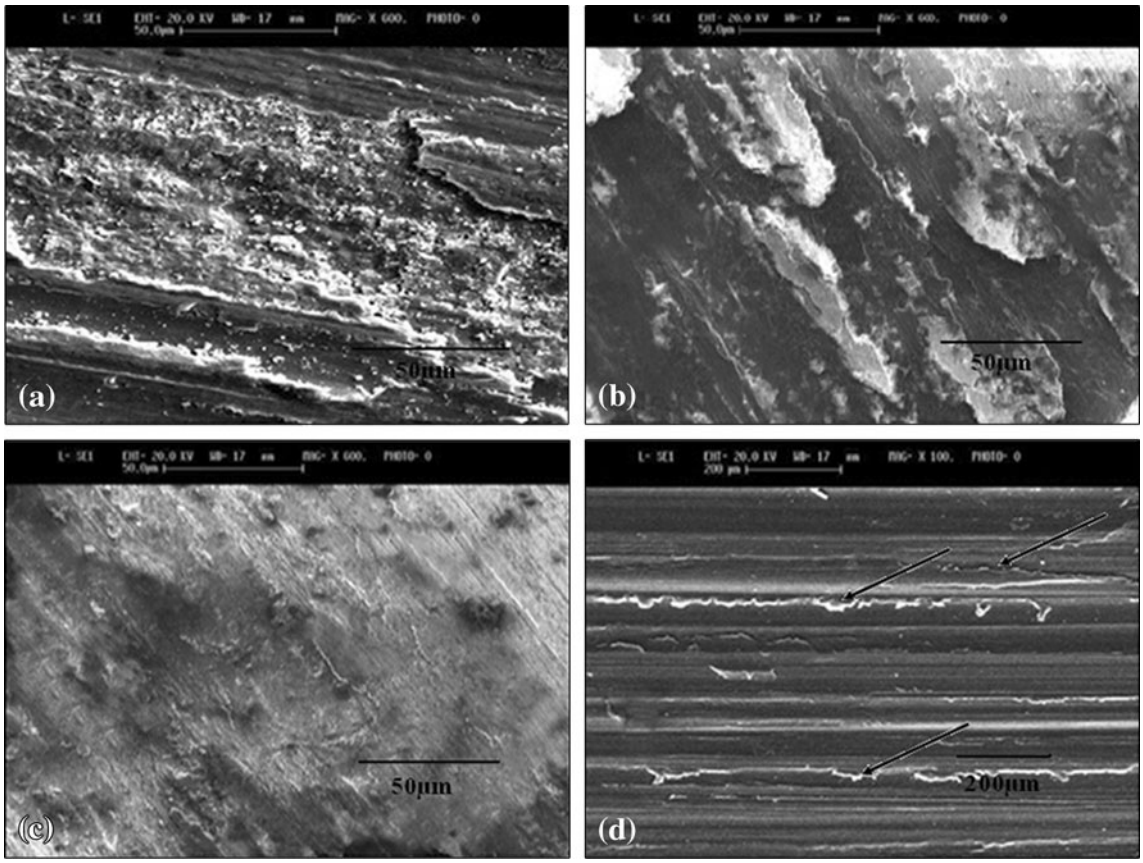

Fig. 8 The SEM micrograph of the worn surface of the nano-composite after (a) first pass of ECAP, (b) second pass of ECAP, (c) third pass of ECAP, and (d) extrusion for the load of 20 N and the sliding distance of 400 m with the velocity of 0.33 m/s

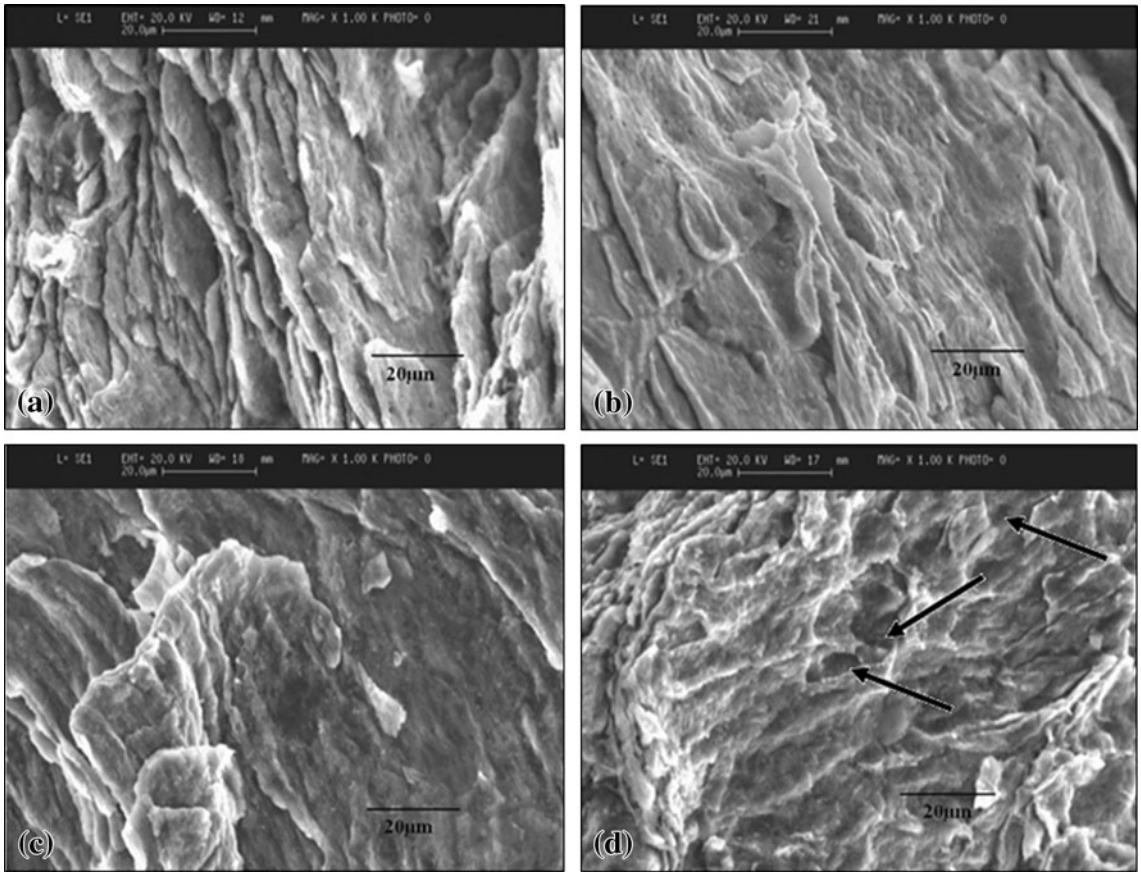

Fig. 9 The fracture surface of the Al-5 vol.% Al_2O_3 composite after (a) first pass, (b) second pass, (c) third pass, and (d) extrusion

of ECAP passes, because of hardness enhancement of the composite, the number of worn particles decreases and in turn causes a decrease in plowing action to the composite surface as Fig. 8(b), (c) shows the SEM micrograph of the worn surface of the nano-composite after the second and the third pass of ECAP, respectively. By comparing the SEM micrograph of the worn surface of the composite after extrusion (Fig. 8d) with the worn surface of the ECAPed samples, it is seen that the microgrooves (solid arrows) due to plowing action have formed on the extruded sample, whereas the worn surface of the composite after the third pass of ECAP has not grooved as much as the extruded sample. This is mainly because of smaller grain size which is obtained after ECAP and also stronger bonds between the reinforcement and the matrix.

Figure 9 demonstrates the fracture surfaces for Al-5 vol.% Al_2O_3 composite after different passes of ECAP and also after extrusion. The fracture surface of the specimen after the first pass of ECAP (Fig. 9a) presents lamellar structure with loose bonds between the plates. However, in the second pass (Fig. 9b) of ECAP, stronger bonds form between the plates and less porosity is observed. Moreover, dispersed shallow dimples are present in the figure. In the third pass (Fig. 9c) due to elimination of the majority of the porosities, local stresses and also particle/matrix decohesion decrease and more homogenous fracture surface is obtained but the river pattern and flat facets which are the signs for cleavage, present a brittle fracture in comparison to the fracture surface of the extruded composite (Fig. 9d) which consists of more dimples that initiate from the nucleation of the microvoids and plastic flow of the matrix that surrounds the nucleation sites and enhances by decohesion of alumina particles (solid arrows in Fig. 9d) in the matrix. Due to this fact that the aluminum matrix in extruded sample has higher ductility because of better plastic flow to initiate the microvoids nucleation site comparing with the aluminum matrix in ECAPed samples, one can observe better ductility in extruded samples.

4. Conclusions

In this study, ECAP of the PIT for increasing the hydrostatic pressure on the powder was used as a technique for consolidation of attritioned aluminum powder (45 μm) with 5 vol.% of nano-alumina powder (35 nm) at 200 °C and the results were compared with the hot extruded 5 vol.% composite. By applying extrusion on the composite, the pressing load increases considerably comparing with the ECAP method. Furthermore, it was found that the mechanical properties of the consolidated composite via ECAP are higher than the extruded composite. The hardness value after three passes of ECAP for the composite improves about 67% comparing with the extrusion method. On the other hand, higher compressive strength of the ECAPed samples and better wear resistance are other features which can be obtained by utilization of ECAP technique. Microstructural investigations show that pores are eliminated gradually by increasing the number of ECAP passes, therefore density of the samples enhances and strong bonds

form between the particles. Optical microscopy demonstrates a 2.5 times smaller grain size after the third pass of ECAP for the composite in comparison to the extruded composite, which improves the ECAPed composites strength and also wear resistance comparing with the extruded samples. An investigation on the fracture surface of the composite demonstrates more homogenous fracture surface with less particle/matrix decohesion after the third pass of ECAP in comparison to the extruded composite.

References

1. H.F. Lee, F. Boey, K.A. Khor, M.J. Tan, J. Gan, and N.L. Loh, The Production of Aluminum Alloy Composites Using a Cold Isostatic Press and Extrusion Approach, *J. Mater. Process. Technol.*, 1992, **29**, p 245–253
2. S.M. Zebarjad and S.A. Sajadi, Dependency of Physical and Mechanical Properties of Mechanical Alloyed Al-Al_2O_3 Composite on Milling Time, *Mater. Des.*, 2007, **28**, p 2113–2120
3. M. Tabandeh Khorshid, S.A. Jenabali Jahromi, and M.M. Moshksar, Mechanical Properties of Tri-Modal Al Matrix Composites Reinforced by Nano- and Submicron-Sized Al_2O_3 Particulates Developed by Wet Attrition Milling and Hot Extrusion, *Mater. Des.*, 2010, **31**, p 3880–3884
4. J.M. Torralba, C.E. da Costa, and F. Velasco, P/M Aluminum Matrix Composites: An Overview, *J. Mater. Process. Technol.*, 2003, **133**, p 203–206
5. B. Prabhu, C. Suryanarayana, L. An, and R. Vaidyanathan, Synthesis and Characterization of High Volume Fraction Al-Al_2O_3 Nanocomposite Powders by High Energy Milling, *Mater. Sci. Eng. A*, 2006, **425**, p 192–200
6. A.A. Mazen and A.Y. Ahmed, Mechanical Behavior of Al-Al_2O_3 MMC Manufactured by PM Techniques Part I—Scheme I, Processing Parameters, *J. Mat. Eng. Perform.*, 1998, **7**, p 393–401
7. A.K. Mukhopadhyay, H.M. Flower, and T. Sheppard, Development of Mechanical Properties in AA 8090 Alloy Produced by Extrusion Processing, *Mater. Sci. Technol.*, 1990, **6**, p 461–468
8. H. Asanuma, M. Hirohashi, and O. Hayama, Fabrication of Complicated Shape Metal Matrix Composites by Combined Extrusion, *Adv. Technol. Plast.*, 1990, **2**, p 945–950
9. M.J. Tan and X. Zhang, Powder Metal Matrix Composites: Selection and Processing, *Mater. Sci. Eng. A*, 1998, **244**, p 80–85
10. A. Parasiris, K.T. Hartwig, and M.N. Srinivasan, Formation/Consolidation of WC-Co Cermets by Simple Shear, *Scripta Mater.*, 2000, **42**, p 875–880
11. K. Xia and X. Wu, Back Pressure Equal Channel Angular Consolidation of Pure Al Particles, *Scripta Mater.*, 2005, **53**, p 1225–1229
12. K. Matsuki, T. Aida, T. Takeuchi, J. Kusui, and K. Yokoe, Microstructural Characteristics and Superplastic-Like Behavior in Aluminum Powder Alloy Consolidated by Equal Channel Angular Pressing, *Acta Mater.*, 2000, **48**, p 2625–2632
13. O.N. Senkov, D.B. Miracle, J.M. Scott, and S.V. Senkova, Equal Channel Angular Extrusion Compaction of Semi-Amorphous Al85-Ni10Y2.5La2.5 Alloy Powder, *J. Alloys. Compd.*, 2004, **365**, p 126–133
14. J. Robertson, J.T. Im, I. Karaman, K.T. Hartwig, and I.E. Anderson, Consolidation of Amorphous Copper Based Powder by Equal Channel Angular Extrusion, *J. Non-Cryst. Solids*, 2003, **317**, p 144–1451
15. I. Karaman, M. Haouaoui, and H.J. Maier, Nanoparticle Consolidation Using Equal Channel Angular Extrusion at Room Temperature, *J. Mater. Sci.*, 2007, **42**, p 1561–1576
16. M.A. Gibbs, K.T. Hartwig, L.R. Cornwell, R.E. Goforth, and E.A. Payzant, Texture Formation in Bulk Iron Processed by Simple Shear, *Scripta Mater.*, 1998, **39**, p 1699–1704
17. M. Haouaoui, K.T. Hartwig, and E.A. Payzant, Effect of Strain Path on Texture and Annealing Microstructure Development in Bulk Pure Copper Processed by Simple Shear, *Acta Mater.*, 2005, **53**, p 801–810
18. A.V. Nagasekhar, Y. Tick-Hon, and K.S. Ramakanth, Mechanics of Single Pass Equal Channel Angular Extrusion of Powder in Tubes, *Appl. Phys. A*, 2006, **85**, p 185–194
19. W. Xu, X. Wu, T. Honma, S.P. Ringer, and K. Xia, Nanostructured Al-Al_2O_3 Composite Formed In Situ During Consolidation of Ultrafine Al Particles by Back Pressure Equal Channel Angular Pressing, *Acta Mater.*, 2009, **57**, p 4321–4330
20. R. Lapovok, D. Tomus, and B.C. Muddle, Low-Temperature Compaction of Ti–6Al–4V Powder Using Equal Channel Angular Extrusion with Back Pressure, *Mater. Sci. Eng. A*, 2008, **490**, p 171–180
21. R. Lapovok, D. Tomus, and C. Bettles, Shear Deformation with Imposed Hydrostatic Pressure for Enhanced Compaction of Powder, *Scripta Mater.*, 2008, **58**, p 898–901
22. M. Balog, F. Simancik, O. Bajana, and G. Requena, ECA vs. Direct Extrusion—Techniques for Consolidation of Ultra-Fine Al Particles, *Mater. Sci. Eng. A*, 2009, **504**, p 1–7
23. P. Quang, Y.G. Jeong, S.H. Hong, and H.S. Kim, Equal Channel Angular Pressing of Carbon Nanotube Reinforced Metal Matrix Nanocomposites, *Key Eng. Mater.*, 2006, **328**, p 325–328
24. R. Derakhshandeh and H.S.A. Jenabali Jahromi, An Investigation on the Capability of Equal Channel Angular Pressing for Consolidation of Aluminum and Aluminum Composite Powder, *Mater.Des.*, 2011, **32**, p 3377–3388
25. Y.T. Zhu and T.C. Lowe, Observations and Issues on Mechanisms of Grain Refinement During ECAP Process, *Mater. Sci. Eng. A.*, 2000, **291**, p 46–53
26. R. Lapovok, Damage Evolution Under Severe Plastic Deformation, *Int. J. Fract.*, 2002, **115**, p 159–172
27. Z. Zhang and D.L. Chen, Contribution of Orowan Strengthening Effect in Particulate-Reinforced Metal Matrix Nanocomposites, *Mater. Sci. Eng. A*, 2008, **483–484**, p 148–152
28. R. Jiang-wei and S. Ai-dang, Strengthening and Stress Drop of Ultrafine Grain Aluminum After Annealing, *Trans. Nonferrous Met. Soc. China*, 2010, **20**, p 2139–2142
29. J.C. Werenskiold, Equal channel angular pressing (ECAP) of AA6082: Mechanical Properties, Texture and Microstructural Development, Ph.D. Thesis, The Norwegian University of Science and Technology, 2004
30. B. Clausen, E. Ustundag, and M.A.M. Bourke, Investigation of the Reduction of $NiAl_2O_4$. JCPDS-International Center for Diffraction Data, *Adv. X-Ray Anal.*, 2001, **44**, p 32–37
31. B. Wielage, T. Muller, and Th. Lampke, Numerical Simulation of Thermo-Elastic Behavior of Textile Structured Ceramic Matrix Composite Bearings, *Int. J. Microstruct. Mater. Prop.*, 2008, **3**, p 65–76
32. V.V. Ganesh and N. Chawla, Effect of Particle Orientation Anisotropy on the Tensile Behavior of Metal Matrix Composites: Experiments and Microstructure-Based Simulation, *Mater. Sci. Eng. A*, 2005, **391**, p 342–353
33. N.B. Dhokey and R.K. Paretkar, Study of Wear Mechanisms in Copper-Based SiC_p (20% by volume) Reinforced Composite, *Wear*, 2008, **265**, p 117–133
34. D.A. Rigney, The Roles of Hardness in the Sliding Behavior of Materials, *Wear*, 1994, **175**, p 63–69